Fabrication and Characterization of a Conductive Proton Exchange Membrane Based on Sulfonated Polystyrenedivinylbenzene Resin-Polyethylene (SPSDR-PE): Application in Direct Methanol Fuel Cells

Mandanipour, Valiollah*[+]

Department of Applied Chemistry, University of Gonabad, Gonabad, I.R. IRAN

Noroozifar, Meissam*[+]

Department of Applied Chemistry, University of Sistan and Baluchestan, P.O. Box 98135-674 Zahedan, I.R. IRAN

Modarresi-Alam, Ali Reza

Polymer Research Laboratory, University of Sistan and Baluchestan, Zahedan, I.R. IRAN

Khorasani-Motlagh Mozhgan

Department of Inorganic Chemistry, University of Sistan and Baluchestan, Zahedan, I.R. IRAN

ABSTRACT: *A novel proton exchange membrane has been prepared using sulfonated poly(styrene-divinylbenzene) resin(SPSDR)–polyethylene(PE). The membrane is characterized by FT-IR, SEM and TGA/DSC. Water uptake, oxidative resistance, ionic conductivity and methanol permeability are measured to evaluate its performance in a direct methanol fuel cell. The on-set degradation temperature of the SPSDR is above 120°C. The membranes were confirmed to retain 1–5% water vapor at 80–140 °C in the air due to the hydrophily of highly sulfonated polystyrene. The ionic conductivity and permeability of the membrane to methanol was found to increase with temperature without extra humidity supply. A direct methanol fuel cell was designed and assembled with the suggested SPSDR-PE membrane. The effect of some experimental factors such as temperature, methanol concentration, and flow rate as well as NaOH concentration on the electrical performances of fuel cells was studied and optimized.*

KEYWORDS: *Sulfonated polystyrene; Polyethylene; Proton exchange membrane; Direct methanol fuel cell; Polymer composites.*

INTRODUCTION

Environmental pollution and energy shortages are priority global concerns. Fuel cell technology is a promising solution to these challenges because final products are electricity and water if hydrogen is applied as the fuel [1]. The Direct Methanol Fuel Cell (DMFC) has such advantages as compact size, low temperature

* *To whom correspondence should be addressed.*
+ E-mail: valimandanipoor@yahoo.com & mnoroozifar@chem.usb.ac.ir
1021-9986/2017/5/151-162 12/$/6.20

the operation, high energy density, rapid startup, environment-friendly, and operation without the combustion of petroleum [2-7]. They are alternative green energy sources for automotive, stationary, and portable equipment [8-11].

Proton exchange membrane (PEM) fuel cell stacks are applied in many fields, such as space shuttles, automobiles, and sub-water devices [12-16]. One of the main problems which limiting performance of direct methanol fuel cell is the high permeability of most common polymeric fuel cell membrane such as Nafion® to methanol. Nafion® membranes due to high proton conductivity, good mechanical properties, and chemical stability under typical fuel cell operating condition are commonly used as fuel cell membrane materials [17-19]. However, Nafion® is very expensive due to an expensive flurination step and lengthy preparation required for manufacturing, and at temperature above 80 °C they lose proton conductivity because of the Nafion® content the low moisture at high temperature and Nafion® have a high methanol diffusion,[3] Therefore, the PEM requires a stronger barrier property for long time operation. Upon this background, many researchers have focused on developing new materials for proton exchange membrane such as poly(arylene ether ketone sulfone), [2] poly(arylene ether sulfone), [3] polystyrene-block-poly(ethylene-ran-butylene)-block-polystyrene, [4] poly(5-vinyl tetrazole) and sulfonated polystyrene, [8] polybenzimidazoles [19] sulfonated polystyrene/acrylate, [20] polyvinylidene fluoride [21].

In this work, we prepared composite sulfonated poly(styrene-divinylbenzene) resin (SPSDR)–polyethylene(PE) membrane and characterized their properties as PEMs. These composite membranes have several advantages over the commercial Nafion® membrane including high proton conductivity, lower methanol permeability, lower membrane cost, and higher selectivity. sulfonated poly(styrene-divinylbenzene) resin–polyethylene (SPSDR-PE) membranes have a hydrophobic polyethylene(PE) and poly(styrene-divinylbenzene) (SPSD) backbone and hydrophilic sulfonic acid (SO_3^-) ionic groups, The SO_3^- are bound to the material structures and difficult to move, and there is an attraction between the H^+ and SO_3^- for each $SO_3^-H^+$. The hydrophilic clusters with $SO_3^-H^+$ can absorb large quantities of water to form hydrated hydrophilic regions. In the hydrated hydrophilic regions, the H^+ is relatively weakly attracted to the SO_3^- and can move more easily. The hydrated hydrophilic regions can be considered as dilute acids, explaining why the membrane needs to be well hydrated (hydrated regions must be as large as possible) for appreciable proton conductivity, and the SO_3^- can be considered as the proton exchange sites since the H^+ often move between the SO_3^-. The water absorption level of ionomer is often represented as the number of water molecules per SO_3^- referred to as the water content. The thickness of the present composite membrane 180 µm and the size of the hydrophilic region that can contain water is on the level of a nanometer. This PEM fuel cell was shown in Fig. 1.

In the present study, we chose poly(styrene-divinylbenzene) resin–polyethylene (SPSDR-PE) as the membrane forming a polymer. The main advantages of using LDPE are that (1) polyolefin copolymers generally have excellent bulk physical/chemical properties; (2) it is inexpensive in comparison with fluoropolymers; (3) it is relatively stable towards alkaline conditions [5]. One of the promising features of the PE-based Anion-Exchange Membranes (AEMs) is their almost complete insolubility in methanol [5], SPSDR-PE is an inexpensive thermoplastic elastomer with excellent mechanical flexibility and chemical stability. There are several literature reports demonstrating the application of sulfonated polystyrene in fuel cells [4, 8, 17, 20, 22, 23].

In this work, several parameters, such as the water content, the proton conductivity of the membrane, the methanol permeability of the membrane, the selectivity of the membrane, were tested. The optimum membrane was investigated and assembled DMFC and the fuel cell polarization curves were plotted for the mentioned DMFC.

EXPERIMENTAL SECTION

Material

All materials and reagents such as methanol (99.9 %), H_2PtCl_6, p-Xylene, NaOH, $NaBH_4$ and polystyrenedivinylbenzene sulfonic acid resin (SPSDR) with surface area = 53 m^2/g, average pore diameter 300 Å, resin capacity 4.7 eq/L were purchased from Merck Company and used without further purification. Multiwall Carbon NanoTubes (CNT), with nanotube diameters, OD = 20-30 nm, wall thickness = 1- 2 nm,

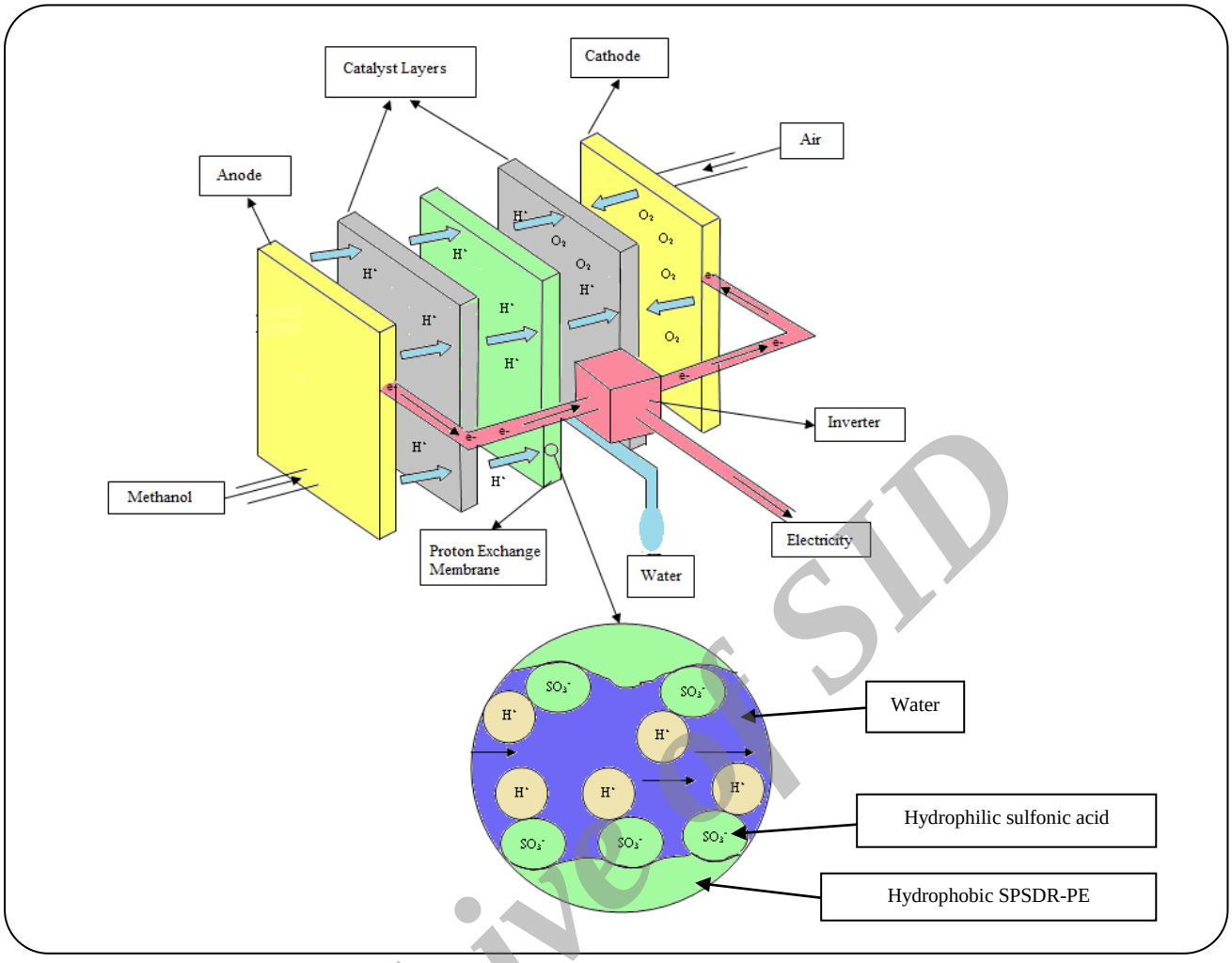

Fig. 1: Schematic of PEM fuel cell.

length = 0.5-2 mm and purity > 95% was purchased from Aldrich. CH ([2-amino-2-deoxy-(1-4)-β-D-glucopyranose]), with medium molecular weight, 400,000 Da, was purchased from Fluka and used as received. Linear low-density polyethylene (LDPE) with density 0.92 g. cm^3, surface hardness SD48, tensile strength 20 Mpa, linear expansion 20×10^{-5} °C, water adsorption 0.01 %, volume resistivity $10^{16}\Omega$.cm and melting temperature range 120-160 °C was purchased from Bandar Imam Petrochemistry. In order to prepare SPSDR, a planetary ball mill (PM100, RETSCH Co.) was used and 50 g of SPSDR was milled for 3 h at 500 rpm.

Instrumentation

The Fourier Transform InfraRed (FT-IR) spectra of the materials and membranes were taken using a JASCO-460 FT-IR spectrometer. The spectral range was 400-4000 cm^{-1}. The surface morphology and the status of the sample were observed by scanning electron microscopy (SEM) and Energy Dispersive X-ray (EDX) analysis, which was equipped with an SEM instrument (MIRA II LMU, Tescan). Dry membranes were manually fractured after cooling in liquid nitrogen. Specimens were sputter coated with gold (15nm thickness) and imaged on a scanning electron microscopy at 15kV. A thermogravimetric analysis was carried out by a TGA/DSC 1 (Mettler Toledo) at a heating rate of 10 K/min under N_2 atmosphere at a flow rate of approximately 50 mL/min.

Preparation of membrane

In order to make thin composite membranes suitable for DMFC application, the goal of the present study is to control composite structure through the application of solvent casting. The solvent casting process involves

evaporating solvent from a polymer solution and is commonly employed to create thin polymeric and polymer composite fuel cell membrane.

For the preparation of the membrane, at first step two solutions were prepared as follow: (1) 1 g of LDPE was dissolved in 25 ml p-Xylene and stirred at 300 rpm for 1.0 h and 100 °C to form a homogeneous solution and (2) 1 g of SPSDR dissolved in p-Xylene to give a yellow polymer solution. In the second step, these two solutions were mixed with each other and homogenized. In the third step, this solution cast on glass plates and dried at 45 °C for 24 h and then at 75 °C in a vacuum for 12 h. The membranes were peeled off, and designated as (SPSDR-PE).

Fuel cell operation

A commercially available catalyzed Carbon Cloth-Diffusion Layer (CC-DL) platinum-ruthenium alloy with a 5 cm^{-2} active area and catalyst loading of 2.0 mg/cm^2 (H_2 Engine Company, manufacturing & development Isfahan science and technology town, Isfahan, Iran) was used as the cathode for the fuel cell experiments. The anode catalyst loading was PtNPs (4.0 mg/cm^2)-CNTs (0.6 mg/cm^2) onto a commercial CC-DL (4.0PtNPs-0.6CNT/CC-DL). The membrane electrode assembly (MEA) for the low-temperature fuel cell was fabricated from SPSDR-PE. The anodic catalyst ink was sprayed uniformly onto the Carbon Cloth-diffusion Layer (CC-DL) using the airbrush kit (model MBD-116C). Both the anode and cathode electrodes were hot-pressed onto both sides of a SPSDR-PE at 100°C and 20 kg cm^{-2} for 30 seconds. The MEA was then cooled down to RT and assembled in the 5 cm^2 single cell for performance evaluation and stability studies. The flow rate of methanol was controlled by a peristaltic pump. I–V curves were obtained galvanostatically with an electronic load, EL200P, Daegil, and controlled by a personal computer. The fuel cell was operated at different condition. Current-voltage data for the first 1-2 h of fuel cell operation reflected the initial performance of the membrane in a DMFC. The performance testing for the single DMFC was started after the fuel cell was stable for 1-2 h of fuel cell operation.

Evaluation of membrane properties

In order to understand the enhanced performance of the proposed membrane, as a proton exchange membrane component, different properties such as water uptake rate, methanol permeability and selectivity factor had major effects and must be measured.

The water uptake of the composite membrane was determined by measuring the change in the weight before and after the hydration. The membrane was first immersed in double distilled water (DDW) for 24 h. Then, the membrane was weighted quickly after removing the surface water to determine the wetted membrane weight (W_{wet}). The dry membrane weight (W_{dry}) was determined after drying the membrane at 373 K for 2 h. The water uptake was calculated with the following equation [24]:

$$\text{Water uptake (\%)} = \frac{Wwet - Wdry}{Wdry} \times 100 \quad (1)$$

The proton conductivity of the membrane was measured using a four-probe method [25] by Electrochemical Impedance Spectroscopy (EIS) with a Zahner potentiostate/galvanostatate electrochemical workstation model PGSTAT over a frequency range of 4MHz-1Hz with the oscillating voltage of 5 mV. For this four-probe method, two inner platinum (Pt) wires (0.2 mm diameter) served as voltage sensors and two outer Pt wires (0.2 mm diameter) served as AC current injectors. The membrane sample, with the size of ca. 3×1.0 cm^2, was sandwiched between two Teflon blocks and held in place with nylon screws. Before the test, the membranes were immersed in a 1.0 M HCl solution for 12 h for activation and then washed with deionized water until pH=7. The proton conductivity measurements were carried out in the temperature range from 30°C in liquid water. Proton conductivity was calculated from the impedance data according to the following: The proton conductivity (s) was calculated according to the following equation:

$$\sigma = \frac{L}{RWd} \quad (2)$$

where σ is the proton conductivity (S/cm), L is the distance between potential-sensing electrodes (cm), R is the membrane resistance R is the resistance associated with the ionic conductivity of a membrane from the impedance data (Ω), W is the width of the membrane (cm) and d is the thickness (cm) of the membrane.

The methanol permeability through the membrane was measured using a custom-built two-compartment diffusion cell. The membrane was clamped vertically between two glass compartments; each compartment contained a magnetic stirring bar for solution agitation. The feed compartment was filled with 5 M methanol, and the receiving chamber contained deionized water. The methanol concentration of the solution in the receiving compartment was measured with a SAMA500 Electroanalyser [26]. The membrane permeability was calculated by the following equation [27]:

$$P = \frac{1}{CA}\left(\frac{\Delta C_{B(t)}}{\Delta t}\right)\left(\frac{L V_B}{A}\right) \quad (3)$$

where P is the methanol diffusion permeability of the membrane ($cm^2\ s^{-1}$), C_A is the concentration of methanol in cell A (mol L^{-1}), $DC_{B(t)}/Dt$ is the slope of the molar concentration variation of methanol in cell B as a function of time (mol/L.s), V_B is the volume of each diffusion reservoir (cm^3), A is the membrane area (cm^2) and L is the thickness of the membrane (cm).

Finally, the selectivity factor (the ratio of the proton conductivity to the methanol permeability) was determined by the following equation [27]:

$$\text{Selectivity} = \frac{\sigma}{P} \quad (4)$$

RESULTS AND DISCUSSION

SEM characterization

A camera picture of SPSDR-PE was shown in Fig. 2a. The membrane's color is yellow. SEM provided information about the morphology of the membrane. The SEM measurements were used to characterize the structure of the membrane. Fig. 2b and c show that surface and cross-sectional micrographs of the SPSDR-PE composite membranes, suggesting that the synthesized films were homogeneous and hence formed a more dense membrane.

FTIR characterization

FT-IR spectra of the SPSDR-PE, SPSDR, and PE are a presence in Fig. 3. Main bands of polyethylene in the IR region are; CH_2 asymmetric strong stretching in 2921 cm^{-1}, CH_2 symmetric strong stretching in 2851 cm^{-1}, bending strong deformation in 1471 and 1463 cm^{-1}, wagging

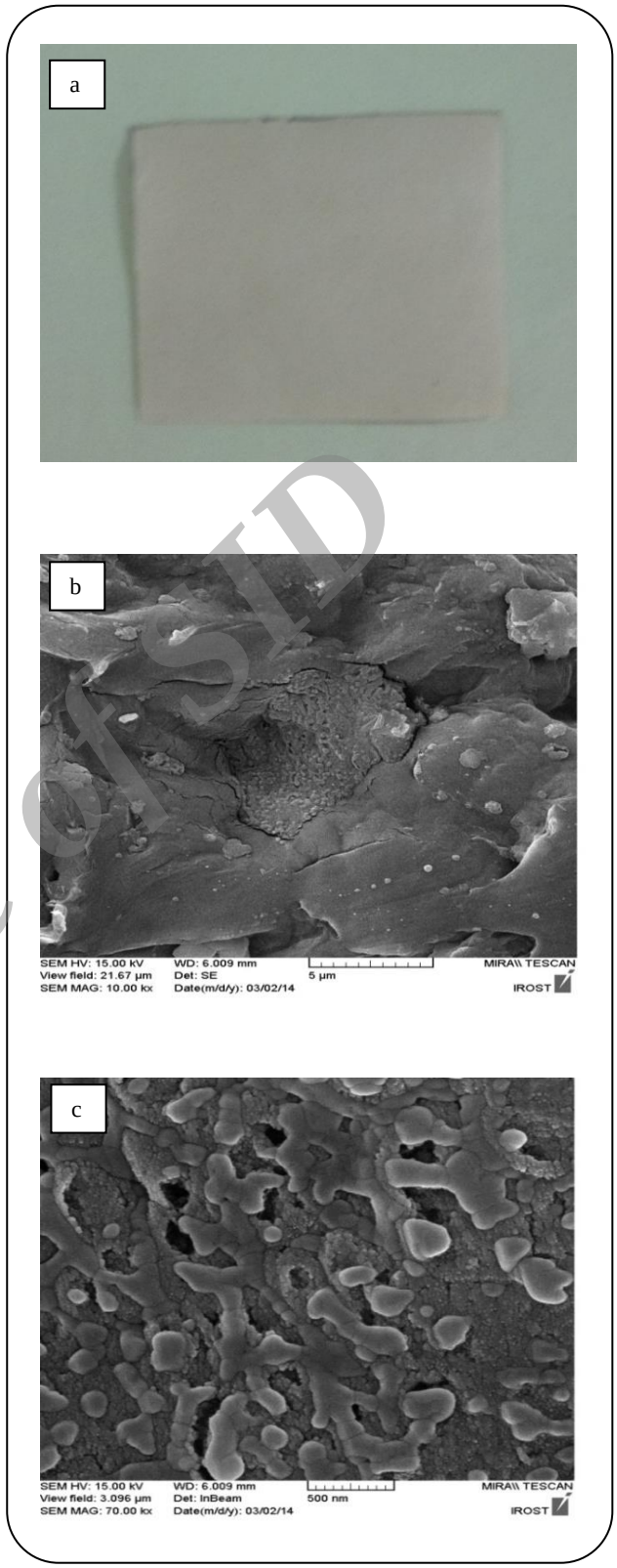

Fig 2. (a) A camera picture of SPSDR-PE membrane, (b) and (c) SEM image for (SPSDR)(PE) membrane with different magnification.

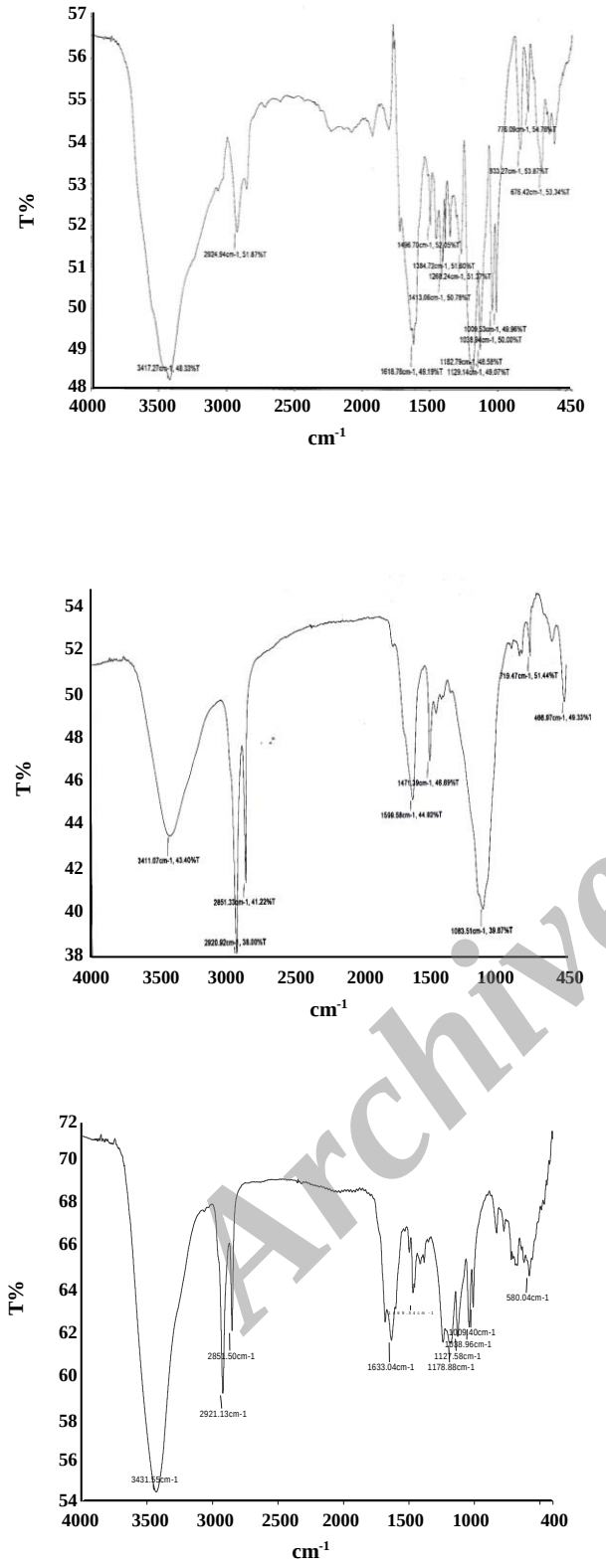

Fig. 3: FT-IR of (a) SPSDR, (b) PE and (c) SPSDR-PE.

medium deformation in 1366 and 1351 cm^{-1}, twisting weak deformation in 1306 cm^{-1}, wagging very weak deformation in 1176 cm^{-1} and rocking medium deformation in 731–720 cm^{-1}. Fig. 3 shows the FT-IR spectrum of the fresh resin sample crosslinked PSD-SO_3H. The bands at 2925 and 2876 cm^{-1} are due to the aliphatic C-H stretching absorbance of methylene and methyne groups in the main chain. SO_2 asymmetric stretching appears at 1385 cm^{-1}. The strong band at 1652 cm^{-1} indicates aromatic C=C bond. The four sharp peaks at 1009 cm^{-1}, 1039 cm^{-1}, 1129 cm^{-1}, 1183 cm^{-1} are due to SO_3 symmetric stretching. The peaks at around 1619 cm^{-1} are due to deformation and skeletal vibrations of C-H in divinylbenzene. The bonding of the sulfonic groups to the aromatic ring of crosslinked PSD-SO_3H is found at 833 cm^{-1} (out of plane deformation bands assigned to substituted aromatic ring γ (Car-H)). The FT-IR spectrum obtained to confirm the structure of the crosslinked PSD-SO_3H-PE membrane. The strong peak centered at 3432 cm^{-1} can be attributed to the stretching vibration of the acid O-H groups. The strong peaks at 2852 cm^{-1} and 2921 cm^{-1} corresponds to the C-H stretching vibration of CH_2 groups. The medium peak centered at 1633 cm^{-1} can be attributed to the stretching vibration of the C=C groups of benzenes. The medium peak centered at around 1469 cm^{-1} can be attributed to the bending vibration of the CH_2 groups and C=C aromatic groups. The four sharp peaks at 1009 cm^{-1}, 1039 cm^{-1}, 1128 cm^{-1}, 1179 cm^{-1} show clearly SO_3 symmetric stretching as above described [27].

Membrane properties measurements

Fig. 4 was shown the water content of Nafion®117 and composite membranes equilibrated with 100% relative humidity air at 25 ˚C and immersed in liquid water at 25 ˚C. As shown in Fig. 4, the water content was higher in the composite membrane (41.67%) than in Nafion®117 (35.52%) which is closed with the literature [27]. The composite membranes had a higher water uptake compared with the commercial Nafion®117 membranes. The water content is important for the ion transportation in the membrane, so a higher water uptake may improve the performance of a fuel cell. The water content in membranes is related to the number of available ion exchange sites and has a profound effect on mechanical properties and ionic conductivity. High water

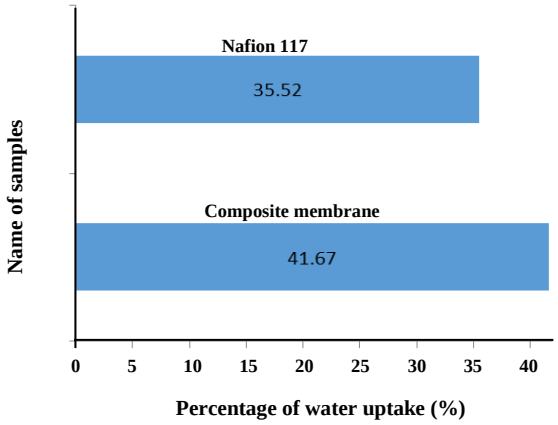

Fig 4: Water uptake of composite and Nafion® 117 membranes.

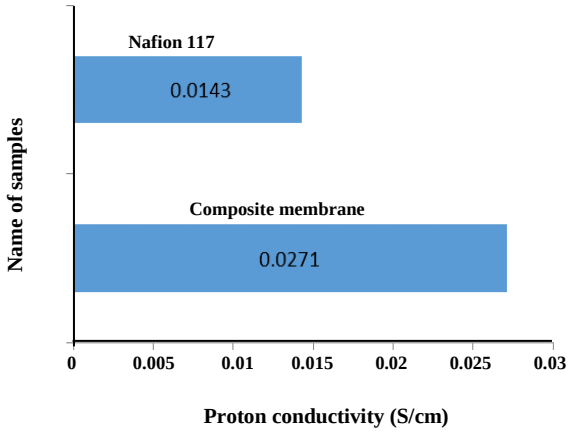

Fig 5: Proton conductivity of wet samples of membranes at room temperature.

content generates solvated ionic species and facilitates their migration by broadening the ion transfer channels, which is necessary for high conductivity. Swelling can also impart mechanical stress on the membranes that can lead to fuel cell device failure.

The proton conductivity of membrane sample was measured at RT and 100% relative humidity. We also tested composite membrane with water for one full day. Fig. 5 shown the proton conductivity of the Nafion® 117 which is closed with the literature [28] and a composite membrane. The proton conductivity of fuel cell membranes is closely related to water content capacity. Swelling of the membranes with water is a requirement for proton conductivity.

Methanol can be used as fuel in solid electrolyte fuel cells, thus measuring methanol permeability is one of the key parameters to evaluate the AEM for fuel cells application. Methanol permeability is the product of the diffusion coefficient and the sorption coefficient and is used to describe the transport of methanol through membranes. Diffusion or leakage of the fuel across the membrane from anode to cathode leads not only to power loss from mixed potentials, but also other undesirable consequences, such as complicated water and thermal management. Thus, high methanol crossover is a serious obstacle for membranes in DMFC applications. the methanol permeability of membrane sample was measured at RT using a 5 M methanol solution. Table 1 shown that methanol permeability in the composite membrane was lower than Nafion®117 which is closed with the literature [28] and selectivity factor for composite membrane was very better than Nafion®117.

The selectivity factor results are shown in Table 1. A membrane with low methanol permeability is advantageous for DMFC usage. Because increasing the proton conductivity and decreasing the methanol permeability is the goal of DMFC membranes. The selectivity factor, proton conductivity/ methanol permeability, can be treated as a guide for developing better DMFC membrane characteristics [29]. The higher selectivity factor contributes to better DMFC performance.

Thermal analysis techniques (TG-DSC) characterizations

Fig. 5 was shown the TGA and DSC curves for SPSDR-PE. The SPSDR-PE membrane exhibit eight weight-loss zones degradation zone (Fig. 6). The parameters associated with this weight-loss region are similar to those observed in the TGA and DSC of SPSDR-PE. Based on Fig. 6, the first weight-loss region is centered around 105–140 °C. It is well known that membrane strongly absorbs water, so this weight loss may be attributed to the loss of absorbed water. The second main weight-loss regions are located around 421-480 °C for SPSDR-PE. Weight losses of 47–57% occur in this region. This weight-loss zone seen is associated with the greatest mass loss and is termed, therefore, the main stage. Therefore, this mass loss has been attributed to the complete thermodegradation of

Table 1: Proton conductivity, methanol permeability and selectivity factor of Nafion® 117 and composite membrane.

Name of samples	Proton conductivity σ (S/cm)	Methanol permeability P (cm^2/s)	Selectivity factor σ/ P ($S.s/cm^3$)
Nafion® 117	1.43×10^{-2}	2.83×10^{-6}	5.05×10^{3}
Composite membrane	2.72×10^{-2}	8.92×10^{-7}	3.05×10^{4}

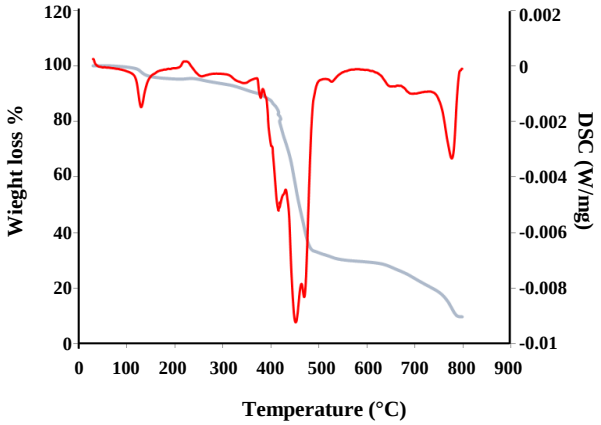

Fig 6: TGA (—) and DSC(—) analysis of the membrane in a temperature range from 30 to 800 °C for SPSDR-PE.

the skeletal chain structure of composite. The weight loss occurring above 650 °C for SPSDR-PE can be used for the elimination of organic moieties. So, the weight loss within a range 650–800 °C is due to the decomposition of the Polystyrenedivinylbenzene .

Single cell performances

In order to understand the performance of the proposed membrane, single cell tests are carried out for the SPSDR-PE membrane for CH_3OH/O_2. The performance of the proposed single cell system depends on composition of membrane, the efficiency of the electrochemical reaction at the interface between the solid phase of electrodes (anode and cathode) and liquid and gas phases in anode and cathode sides, concentration of NaOH in carrier stream, methanol concentration of carrier stream, temperature and flow rate of fuel had major effects [30] and must be optimized.

The anodic and cathodic reactions (AR and CR) in the fuel cell are given by Eq. 5 and 6;

$$\text{Anodic;}\quad CH_3OH + H_2O \rightarrow CO_2 + 6H^+ + 6e^- \qquad (5)$$

$$\text{Cathodic;}\quad \frac{3}{2}O_2 + 6e^- + 6H^+ \rightarrow 3H_2O \qquad (6)$$

In a DMFC, H^+ ions transfer from anodic side to cathodic side by passing through a Cation exchange membrane (CEM) and the overall reaction is Eq. 7;

$$CH_3OH + \frac{3}{2}O_2 \rightarrow CO_2 + 2H_2O \qquad (7)$$

There are two major problems such as the high costs of CEMs and precious metal catalysts (Pt and Pt/Ru based catalysts) as well as CO poisoning of Pt catalysts at lower temperatures which in acidic media have further hampered the development of DMFCs. It is known that for many reactions, electrocatalysts perform better in alkaline electrolytes so that both passive DMAFC with AEM and CEM have been worked in alkaline media. In the case of DMAFC, the AR and CR are as follow;

$$\text{Anodic;}\quad CH_3OH + 6OH \rightarrow CO_2 + 5H_2O + 6e^- \qquad (8)$$

$$\text{Cathodic;}\quad \frac{3}{2}O_2 + 3H_2O + 6e^- \rightarrow 6OH^- \qquad (9)$$

and overall reaction is Eq. 10:

$$CH_3OH + \frac{3}{2}O_2 \rightarrow CO_2 + 2H_2O \qquad (10)$$

In the case of a passive DMAFC with CEM; as NaOH solution is added to the methanol reservoir, hydroxide anions (OH^-) will be formed at the anode electrode according to Eq. 11;

$$NaOH \rightarrow Na^+ + OH \qquad (11)$$

Therefore, the methanol reacts with hydroxide ions that exist in methanol/alkali solution in reservoir according to Eq. (8). For DMAFC with CEM at the cathode, there exist two reactions: i) O_2 reacts with water and the electrons to produce OH^- according to Eq. (9) and ii) the produced OH^- combines with a migrated cation (Na^+) through the membrane to form the alkali salt (NaOH) [31]. The NaOH concentration as fuel has a significant effect on electrical performances such as cell voltage and power density, as one would expect.

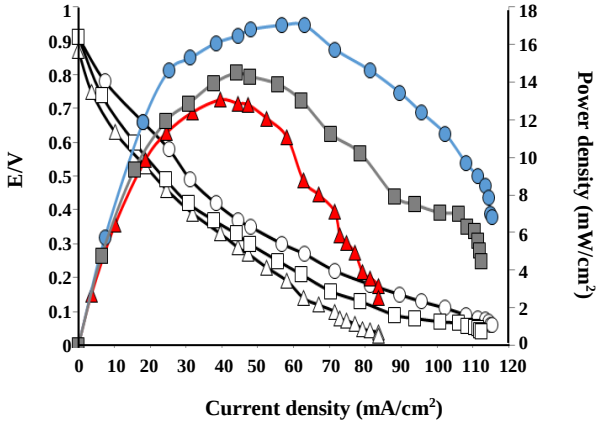

Fig. 7: Polarization curves (Cell voltage against current density and power density against current density) of a 5 cm² DMFC with different concentration of NaOH(▲) 1.0, (●) 2.0 and (■) 3.0 (M) using the P_{O_2}= 2 bar, [Methanol] = 2.0 M, flow rate = 1.6 mL/min, Temperature = 80 °C.

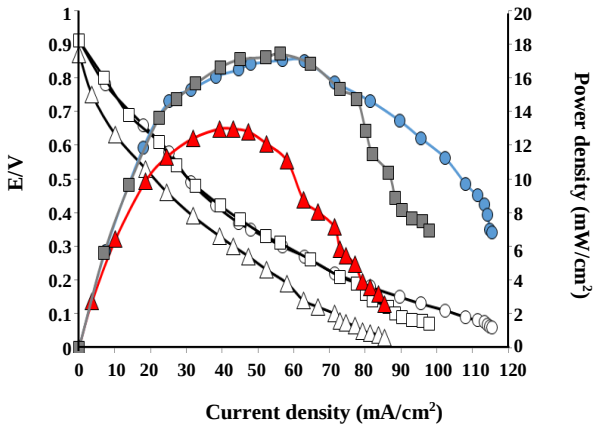

Fig. 8: Polarization curves (Cell voltage against current density and power density against current density) of a 5 cm² DMFC with different concentration of methanol (▲) 1.0, (●) 2.0 and (■) 3.0 (M) using the P_{O_2}= 2 bar, flow rate = 1.6 mL/min, Temperature = 80 °C, NaOH= 2.0M.

The polarization curves of the single cell system were studied for various NaOH concentrations in the range 1 and 3 M. The results were shown in Fig. 6. The OCV increased with an increase of the NaOH concentration from 1 to 2 M and then decrease with increasing concentration to 3M. Based on the results, a 2 M NaOH concentration was chosen as optimum.

The methanol concentration as fuel has a significant effect on electrical performances such as cell voltage and power density, as one would expect. The polarization curves of the single cell system were studied for various methanol concentrations. Fig. 7 shows the results for proposed DMFC in 1 and 3 M methanol concentration. The OCV increased with an increase of the methanol concentration from 1 to 2 M and then decrease with increasing concentration to 3M. Based on the results, a 2 M methanol concentration was chosen as optimum. In order to investigate the effect of temperature on the performance of fuel cell, a various temperature ranging from 60-90 °C were tested while keeping [methanol] constant at 2M with flow rate 1.6 mL/min, [P_{O_2}] 2 bar. The results were shown in Fig 8. From the I–Vcharacteristics, the maximum power density of the single cells using the SPSDR-PE membrane was obtained at 80°C. Based on the results, 80 °C was chosen as optimum for DMFC temperature. Finally, the flow rates have a significant effect on the I–V characteristics and the OCV of the single cell. The results of the system were studied for various flow rates: 1.0, 1.6 and 2.3 mL/min.The results were shown in Fig. 9. As can be seen, the optimum flow rates were 1.6 mL min^{-1} for the proposed fuel cell.

CONCLUSIONS

SPSDR composite in PE was synthesized by a simple method. Characterizations of the composites were carried out using FT-IR, SEM techniques, and TGA/DSC. At higher temperatures, conductivity increases because of hopping of polarons from one localized states to another localized states. The TGA-DSC curve confirmed the thermal stability of composite. A direct methanol fuel cell was designed, assembled and tested with suggested SPSDR-PE composites under several different conditions. The effect of experimental factors such as temperature, methanol concentration, and flow rate as well as NaOH concentration on the electrical performances of the fuel cell were studied and optimized. Selected optimizations of the experimental conditions for a proposed membrane with various membranes are listed in Table 2. The power density (18 $mW.cm^{-2}$) at the SPSD-PE for DMFC is considerably better than those described in the literature for different membranes such as Nafion 117 [27], nafion-zirconium phosphate [27], special-shaped direct methanol fuel cell [32] and Nafion-Polyaniline – Silica [33].

Table 2: Comparison the proposed DMFC with SPSD-PE membrane with other DMFCs with different membranes.

Membrane	Membrane size / cm^2	Anode loading/ Mg/cm^2	Cathode loading/ Mg/cm^2	Temperature/ °C	Methanol concentration/ M	Power Density/ mW/cm^2	Ref.
Nafion 117	4	8- Pt/Ru	8- Pt	RT	5	8.6	[27]
Nafion-ZP [a]	3	1-1.25- Pt/Ru	5- Pt	RT	1	6-8	[27]
SDMFC [b]	4	3- 40% Pt/20% Ru/C	1.75- 40% Pt/C	60	1	9.4	[32]
Nafion- Polyaniline - Silica	5	4- 80 wt% Pt/Ru on carbon	4- Pt	40	2	8	[33]
SPSD -PE	5	4.0-PtNPs-0.6-CNTs/CC-DL	2- Pt	80	2	18	This work

[a] *zirconium phosphate (ZP),* [b] *special-shaped direct methanol fuel cell.*

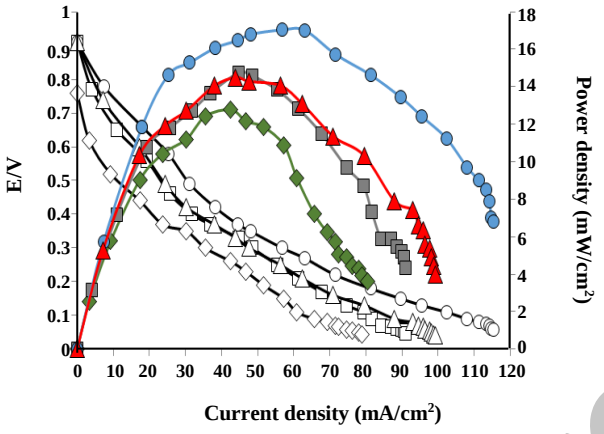

Fig. 9: Polarization curves (Cell voltage against current density and power density against current density) of a 5 cm^2 DMFC with different temperature (♦) 60.0, (■) 70.0, (●) 80.0 and (▲) 90.0 (˚C) using the Po_2= 2 bar, [Methanol] = 2.0 M, flow rate = 1.6 mL/min,and NaOH= 2.0M.

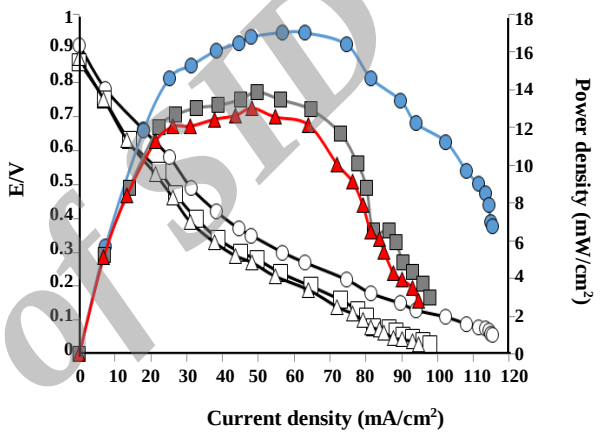

Fig. 10: Polarization curves (Cell voltage against current density and power density against current density) of a 5 cm^2 DMFC with different fuel flow rates (▲) 1.0, (●) 1.6 and (■) 2.3 (mL/min) using the Temperature = 80 °C,Po_2= 2 bar, [Methanol] = 2.0 M, and NaOH= 2.0M.

Acknowledgments

We thank University of Sistan and Baluchestan (USB) for financial support.

Received : Dec. 17, 2015 ; Accepted :May 22, 2017

REFERENCES

[1] Zhang L., Chae S-R., Hendren Z., Park J-S., Wiesner M.R., Recent Advances in Proton Exchange Membranes for Fuel Cell Applications, *Chem. Eng. J.*, **204**: 87–97 (2012).

[2] Xu J., Ma L., Han H., Ni H., Wang Z., Zhang H., Synthesis and Properties of a Novel Sulfonated Poly(arylene ether ketone sulfone) Membrane with a High β-value for Direct Methanol Fuel Cell Applications, *Electrochim. Acta*, **146**: 688–696 (2014).

[3] Kim D.J., Lee H.J., Nam S.Y., Sulfonated Poly(arylene ether sulfone) Membranes Blended with Hydrophobic Polymers for Direct Methanol Fuel Cell Applications, *Int. J. Hydrogen Energy*, **39**: 17524-17532 (2013),.

[4] Zeng Q.H., Liu Q.L., Broadwell I., Zhu A.M., Xiong Y., Tu X.P., Anion Exchange Membranes Based on Quaternized Polystyrene-block-poly(ethylene-ran-butylene)-block-polystyrene for Direct Methanol Alkaline Fuel Cells, *J. Membr. Sci.*, **349**: 237–243 (2010).

[5] Sherazi T.A., Sohn J.Y., Lee Y.M., Guiver M.D., Polyethylene-based Radiation Grafted Anion-Exchange Membranes for Alkaline Fuel Cells, *J. Membr. Sci.*, **441**: 148–157 (2013).

[6] Liu W., Cai W., Liu C., Sun Sh., Xing W., Magnetic Coupled Passive Direct Methanol Fuel Cell: Promoted CO_2 Removal and Enhanced Catalyst Utilization, *Fuel*, **139**: 308-313 (2015).

[7] Liang X., Pan G., Xu L., Wang J., A Modified Decal Method for Preparing the Membrane Electrode Assembly of Proton Exchange Membrane Fuel Cells, *Fuel*, **139**: 393-400 (2015).

[8] Li J., Wang J., Chen Xi., Lv Zh., Chen T., Wang T., A Highly Conductive Proton Exchange Membrane for High Temperature Fuel Cells Based on Poly(5-vinyltetrazole) and Sulfonated Polystyrene, *Solid State Ionics*, **255**: 128-134 (2014).

[9] Cho M. K., Lee D-N., Kim Y-Y., Han J., Kim H-J., Cho E.A., Lim T-H., Henkensmeier D., Yoo S.J., Sung Y-E., Park S., Jang J.H., Analysis of the Spatially Distributed Performance Degradation of a Polymer Electrolyte Membrane Fuel Cell Stack, *Int. J. Hydrogen Energy*, **39**: 16548-16555 (2014).

[10] Liu J., Laghrouche S., Ahmed F-Sh., Wack M., PEM Fuel Cell Air-Feed System Observer Design for Automotive Applications: An Adaptive Numerical Differentiation Approach, *Int. J. Hydrogen Energy*, **39**, 17210-17221(2014).

[11] Hassan M.A., Kamarudin S.K., Loh K.S., Daud W.R.W., Sensors for Direct Methanol Fuel Cells, *Renew. Sust. Energ. Rev.*, **40**: 1060-1069 (2014).

[12] Luo Y., Jiao K., Jia B., Elucidating the Constant Power, Current and Voltage Cold Start Modes of Proton Exchange Membrane Fuel Cell, *Int. J. Heat. Mass. Tran.*, **77**: 489–500(2014).

[13] Ogden J.M., Steinbugler M.M., Kreutz Th.G., A Comparison of Hydrogen, Methanol and Gasoline as Fuels for Fuel Cell Vehicles: Implications for Vehicle Design and Infrastructure Development, *J. Power Sources*, **79**: 143–168(1999).

[14] Hong-jun N., Cheng-jin Zh., Xing-xing W., Su-yang M., Ping L., Performance of Special-Shaped Direct Methanol Fuel Cell with Sol–Gel Flux Phase, *J. Fuel Chem. Technol*, **38**(5): 604-609 (2010).

[15] Mekhilef S., Saidur R., Safari A., Comparative Study of Different Fuel Cell Technologies, *Renew. Sust. Energ. Rev.*, **16**: 981–989 (2012).

[16] Wang Y., Geder J., Schubert J.M., Dahl R., Pasel J., Peters R., Optimization of Adsorptive Desulfurization Pocess of Jet Fuels for Application in Fuel Cell Systems, *Fuel Process. Technol.*, **95**: 144–153(2012).

[17] Wei X., Yates M.Z., Nafion®/polystyrene-b-poly(ethylene-ran-butylene)-b-polystyrene Composite Membranes with Electric Field-Aligned Domains for Improved Direct Methanol Fuel Cell Performance, *Power Sources*, **195**: 736–743(2010).

[18] Perrot C., Gonon L., Marestin C., Gebel G., Hydrolytic Degradation of Sulfonated Polyimide Membranes for Fuel Cells, *J. Membr. Sci.*, **379**: 207-214 (2011).

[19] Li Q., Jensen J.O., Savinell R.F., Bjerrum N.J., High Temperature Proton Exchange Membranes Based on Polybenzimidazoles for Fuel Cells, *Prog. Polym. Sci.*, **34**: 449–477(2009).

[20] Zhong S., Cui X., Dou S., Liu W., Gao Y., Hong B., Improvement in Silicon-Containing Sulfonated Polystyrene/Acrylate Membranes by Blending and Crosslinking, *Electrochim. Acta*, **55**: 8410–8415 (2010).

[21] Abdrashitov E.F., Bokun V.Ch., Kritskaya D.A., Sanginov E.A., Ponomarev A.N., Dobrovolsky Y.A., Synthesis and Properties of the PVDF-Based Proton Exchange Membranes with Incorporated Cross-Linked Sulphonatedpolystyrene for Fuel Cell, *Solid State Ionics*, **251**: 9-12 (2013).

[22] Díaz M., Ortiz A., Ortiz I., Progress in the Use of Ionic Liquids as Electrolyte Membranes in Fuel Cells, *J. Membr. Sci.*, **469**: 379-396 (2014).

[23] Díaz M., Ortiz A., Isik M., Mecerreyes D., Ortiz I., Highly Conductive Electrolytes Based on Poly([HSO_3 BVIm][TfO])/[HSO_3-BMIm][TfO] Mixtures for Fuel Cell Applications, *Int. J. Hydrogen Energy*, **40**(34): 11294–11302 (2015).

[24] Ahmad H., Kamarudin S.K., Hasran U.A., Daud W.R.W., Overview of Hybrid Membranes for Direct-Methanol Fuel-Cell Applications, *Int. J. Hydrogen Energy*, **35**: 2160-2175 (2010).

[25] Xie Z., Song C., Andreaus B., Navessin T., Shi Z., Zhang J., Holdcroft S., Discrepancies in the Measurement of Ionic Conductivity of PEMs Using Two- and Four-Probe AC Impedance Spectroscopy, *J. Electrochem. Soci.*, **153**(10) : 173-178 (2006).

[26] Khorasani-Motlagh M., Noroozifar M., Ekrami-Kakhki M-S, Investigation of the Nanometals (Ni and Sn) in Platinum Binary and Ternary Electrocatalysts for Methanol Electrooxidation, *0i Int. J. Hydrogen Energy*, **36**: 11554-11563 (2011).

[27] Ahmad H., Kamarudin S.K., Hasran U.A., Daud W.R.W., A Novel Hybrid Nafion-PBI-ZP Membrane for Direct Methanol Fuel Cells, *Int. J. Hydrogen Energy*, **36**: 14668-14677 (2011).

[28] Wang C.-H., Chen C.-C., Hsu H.-C., Du H.-Y., Chen C.-P., Hwang J.-Y., Chend L.C., Shih H.C., Stejskal J., Chen K.H., Low Methanol-Permeable Polyaniline/Nafion Composite Membrane for Direct Methanol Fuel Cells, *J. Power Sources*, **190**: 279-284 (2009).

[29] Mishraa A.K., Boseb S., Kuilab T., Kimc N.H., Lee J.H., Silicate-Based Polymer-Composite Membranes for Polymer Electrolyte Membrane Fuel Cells, *Prog. Polym. Sci.*, **37**: 842– 869 (2012).

[30] Mehdi S., Khaleghi H., Mirzaei M., Parametric Study of Operation and Performance of a PEM Fuel Cell Using Numerical Method, *Iran. J. Chem. Chem. Eng. (IJCCE)*, **27**(2): 1-12 (2008).

[31] Najmi A., Rowshanzamir S., Parnian M., Investigation of NaOH Concentration Effect in Injected Fuel on the Performance of Passive Direct Methanol Alkaline Fuel Cell with Modified Cation Exchange Membrane, *Energy*, **94**: 589-599(2016).

[32] Ni H-J., Zhang Ch-J., Wang Xi-Xi., Ma Su-Y., Liao P., Performance of Special-Shaped Direct Methanol Fuel Cell with Sol-Gel Flux Phase, *J. Fuel. Chem. Technol.*, **38**: 604-609(2010).

[33] Chen C.Y., Garnica-Rodriguez J.I., Duke M.C., Dalla Costa R.F., Dicks A.L., Diniz da Costa J.C., Nafion/Polyaniline/Silica Composite Membranes for Direct Methanol Fuel Cell Application, *J. Power Sources*, **166**: 324-330(2007).